Absolute Configuration of C_2-Symmetric Spiroselenurane: 3,3,3′,3′-Tetramethyl-1,1′-spirobi[3*H*,2,1]Benzoxaselenole

Ana G. Petrovic,[a] Prasad L. Polavarapu,*[a] Jozef Drabowicz,[b, e] Yingru Zhang,[c] Oliver J. McConnell,[c] and Helmut Duddeck[d]

Abstract: The enantiomers of 3,3,3′,3′-tetramethyl-1,1′-spirobi[3*H*,2,1]benzoxaselenole have been separated on a chiral preparative chromatographic column. The experimental vibrational circular dichroism (VCD) spectra have been obtained for both enantiomers in CH_2Cl_2. The theoretical VCD spectra have been obtained by means of density functional theoretical calculations with the B3LYP density functional. From a comparison of experimental and theoretical VCD spectra, the absolute configuration of an enantiomer with positive specific rotation in CH_2Cl_2 at 589 nm is determined to be *R*. This conclusion has been verified by comparing results of experimental optical rotatory dispersion (ORD) and electronic circular dichroism (ECD) to predictions of the same properties using the B3LYP functional for the title compound.

Keywords: circular dichroism · configuration determination · optical rotation · selenuranes · vibrational spectroscopy

Introduction

In the field of organic synthesis, considerable interest[1] has been devoted to the preparation of optically active, spirocyclic, hypervalent compounds containing sulfur, tellurium, or selenium as the central atom. This interest has arisen due to the recognition that, until relatively recently, very few compounds of this kind have been characterized in the optically active form and, therefore, a substantial amount of important stereochemical information has been lacking. Spiroselenuranes constitute a family of hypervalent selenium compounds that exhibit trigonal bipyramidal geometry and display chirality due to molecular dissymmetry. Examples of previously studied spiroselenuranes are 3,3′-spirobi-(3-selenaphthalide) (**1**, see Scheme 1) and its 7-carboxy derivative.

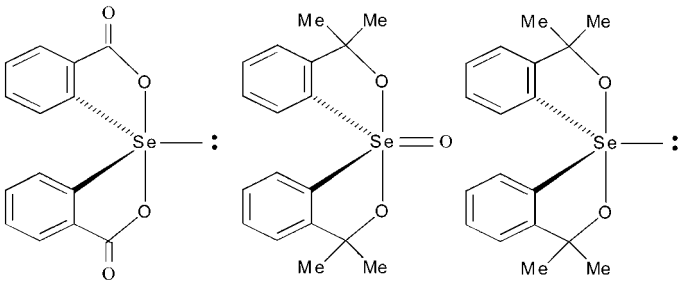

$(-)_{589}$-(*S*)-**1** $(+)_{589}$-(*S*)-**2** $(-)_{589}$-(*S*)-**3**

Scheme 1. The chemical structures of 3,3′-spirobi-(3-selenaphthalide) (**1**), 3,3,3′,3′-tetramethyl-1,1′-spirobi[3*H*,2,1]benzoxaselenole oxide (**2**), and 3,3,3′,3′-tetramethyl-1,1′-spirobi[3*H*,2,1]benzoxaselenole (**3**).

Compound **1** was first synthesized by Lesser and Weiss[2] and the synthesis was later reinvestigated by Dahlen and Lindgren.[3] Okazaki et al.[4] accomplished the synthesis of 1,5-dioxa-4-selenaspiro[3.3]heptanes, a type of spiroselenurane bearing two oxaselenetane rings. Koizumi et al. have prepared[5] a few enantiomerically pure spiroselenuranes and spirotelluranes by using the 2-exo-hydroxy-10-bornyl

[a] A. G. Petrovic, Prof. P. L. Polavarapu
Department of Chemistry, Vanderbilt University
Nashville, TN 37235 (USA)
Fax: (+1) 615-322-4936
E-mail: Prasad.L.Polavarapu@vanderbilt.edu

[b] Dr. J. Drabowicz
Center for Molecular and Macromolecular Research
Polish Academy of Sciences, 93–236 Lodz (Poland)

[c] Dr. Y. Zhang, Dr. O. J. McConnell
Wyeth Research, Collegeville, PA (USA)

[d] Prof. H. Duddeck
Institute of Organic Chemistry, Hannover University
Schneiderberg 1B, 30167 Hannover (Germany)

[e] Dr. J. Drabowicz
Institute of Chemistry and Environmental Protection
Jan Długosz University, ul. Armii Krajowej 13/15
42–200 Czestochowa (Poland)

 DOI: 10.1002/chem.200401331

group as a chiral ligand. Recently, Drabowicz and co-workers have reported[6a] the synthesis and absolute configuration of 3,3,3′,3′-tetramethyl-1,1′-spirobi[3*H*,2,1]benzoxaselenole oxide (**2**, see Scheme 1) and determined its absolute configuration using X-ray crystallography. They have also synthesized[6b] 3,3,3′,3′-tetramethyl-1,1′-spirobi[3*H*,2,1]benzoxaselenole (**3**, see Scheme 1), but its absolute configuration has not yet been determined.

In the light of continued interest in investigating the stereochemistry of hypervalent compounds containing a central selenium atom, the research presented here uses chiroptical methods to determine the absolute configuration and the dominant conformation of **3**. The stereochemical assignments have been previously made for **1** and **2**, which have structural resemblances with **3** (Scheme 1). The enantiomer of **1**, with negative optical rotation at 589 nm, was assigned[1] *S* configuration, while the enantiomer of **2**, with negative optical rotation at 589 nm, has been assigned[6a] *R* configuration. In this manuscript we determine and report the absolute configuration of **3**.

Vibrational circular dichroism (VCD) is an independent spectroscopic method[7] for determining the absolute configuration and dominant conformation(s) in the solution phase. The development of methods[8] for reliably predicting VCD using density functional theory (DFT) and the availability of quantum mechanical programs,[9] in conjunction with the availability of commercial VCD instruments, has facilitated the use of this technique. Numerous examples are now available,[7c] in which VCD has been successfully used to determine the absolute configuration and predominant confirmation(s) in the solution phase.

The first ab initio prediction of optical rotation was reported[10] in 1997 and since then numerous advances[11] have taken place in using optical rotation for structural elucidation. Some reports have also emphasized the use[12] of optical rotatory dispersion (ORD), instead of rotation at one wavelength, for assigning the absolute configuration. Similarly, the development of DFT methods for electronic circular dichroism (ECD)[13] has also led to the use of ECD for establishing the absolute configuration. In particular, the availability of quantum mechanical programs[9] for these calculations has facilitated the applications of ORD and ECD.

In this manuscript, the absolute configuration and predominant conformation of **3** have been determined using experimental and density functional theoretical VCD studies. The conclusions obtained from VCD studies are further supported by experimental and theoretical studies on ORD and ECD. This is the first study where VCD, ORD, and ECD have been used together to establish the absolute configuration.

Results and Discussion

The stereoisomers available to a molecule can have a dramatic effect on its activity and reactivity. In some cases an ensemble of stereoisomers may be responsible for an observed behavior. Therefore, it is important to account for all possible low-energy stereoisomers. The conformational rigidity of **3** restricts the consideration to only two different isomers (Figure 1). Although NMR data for **3** have been reported,[6b] the predominance of one or both of these isomers has not been established. Therefore we investigated the two isomers, *trans* and *cis*, differing in dihedral angle, labeled as D(5-4-1-3). The *trans* isomer, with $D(5\text{-}4\text{-}1\text{-}3) = 5.6°$ (Figure 1a), has C_2 symmetry and was obtained by optimizing the geometry of the structure that possesses coordinates acquired from the spiroselenurane crystal structure.[6b] The *cis* isomer (Figure 1b) considered has no symmetry and is characterized by the dihedral angle $D(5\text{-}4\text{-}1\text{-}3) = -105.6°$. The initial structure for the *cis* isomer was obtained by doing a manual search for possible low-energy conformations.

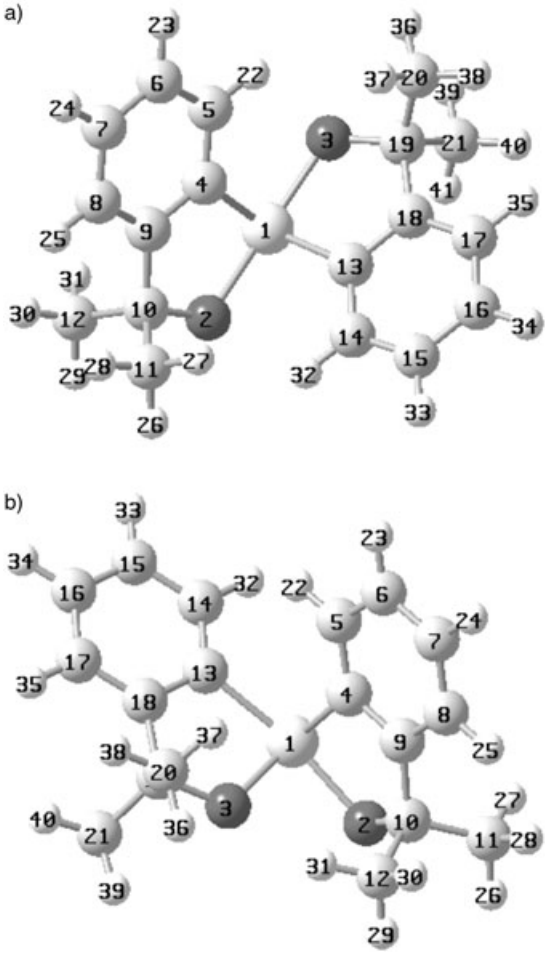

Figure 1. B3LYP/6–31G* optimized structures of two stereoisomers of **3**: a) *trans* isomer with $D(5\text{-}4\text{-}1\text{-}3) = 5.6°$; b) *cis* isomer with $D(5\text{-}4\text{-}1\text{-}3) = -105.6°$.

The converged dihedral angles, optimized electronic energies, and relative populations are listed in Table 1. Due to the rigidity of the spiroselenurane structure, it is not surprising that among the two isomers under consideration only one is dominant. Based on the DFT-predicted electronic en-

Table 1. B3LYP/6–31G* predictions of optimized dihedral angles, energies, and relative populations of the two isomers of **3**.

	Dihedral angle,[a] D(5-4-1-3) [°]	Electronic energy [hartree]	Population [%]
trans isomer	5.6	−3247.76880356	100
cis isomer	−105.6	−3247.73567341	0

[a] See Figure 1 for atom numbering.

ergies, and the relative Boltzmann populations thereby calculated, the *trans* isomer with D(5-4-1-3) = 5.6° is seen to be dominant.

Specification of the absolute configuration[14–16] of the structure used in the theoretical calculation is based on established convention for spirane compounds.[16] To specify the absolute configuration, atoms surrounding the selenium are assigned priority designations (Figure 2). The atoms labeled as "a" and "b" with the same subscripts designate the pair of atoms sharing the same ring. Labels a_1 and a_2 carry higher priority than b_1 and b_2. Placing the lowest priority group (b_2) in the back, away from the observer, and following the sequence a_1-a_2-b_1 gives a clockwise rotation and, hence, *R* configuration for the structure used in the calculations. The same *R* absolute configuration for this structure can be designated by the modification of the Cahn–Ingold–Prelog rules[17] proposed by Martin and Balthazor.[18]

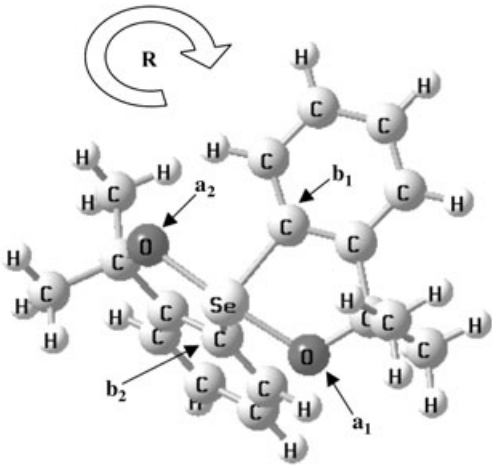

Figure 2. Priority designations aiding the configurational assignment for the structure used in theoretical calculations on **3**.

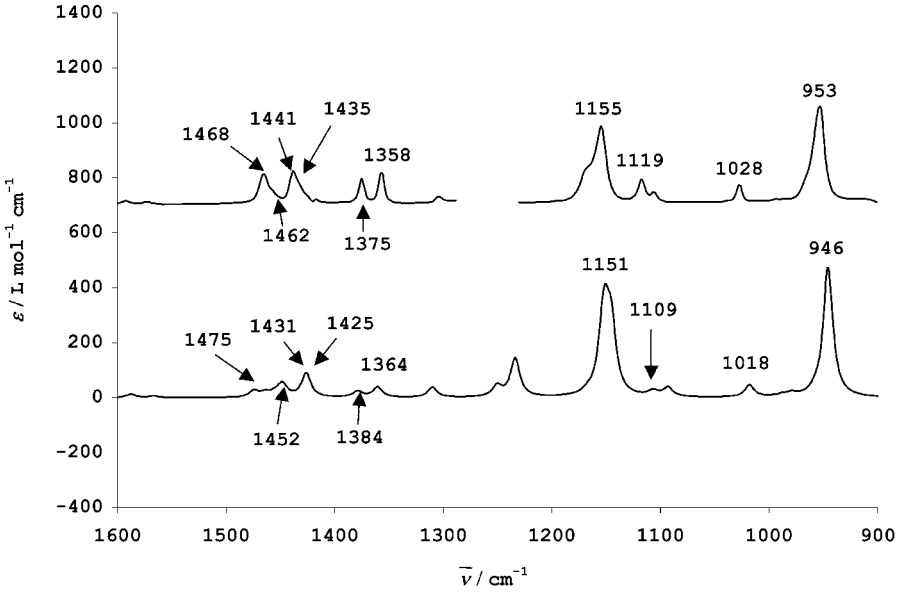

Figure 3. Comparison of the experimental absorption spectrum of (+)-**3** (0.086 M in CH_2Cl_2; path length = 110 μm) with the predicted absorption spectrum (B3LYP/6–31G*) of (*R*)-**3** (top and bottom plots, respectively). Lorentzian band shapes with a half-width at one-half of the peak height of 5 cm^{-1} were used in the spectral simulation; 6–31G* frequencies were scaled by 0.9613.

The theoretical vibrational spectra are compared to the corresponding experimental spectra in Figure 3 and Figure 4. It is well known that the B3LYP/6–31G* calculated frequencies are larger than the observed frequencies and, therefore, need to be scaled. Even after scaling there will be differences between calculated and observed frequencies due to inaccuracies at the level of theory used and due to anharmonic effects in the experimental frequencies. Therefore, the correlation between predicted and experimental spectra is normally made by following spectral patterns (that is, higher-intensity bands in the experimental spectra correspond to higher intensity bands in the predicted spectra, etc.). The region between ~1300 and 1246 cm^{-1} is not shown in the experimental spectra due to interference from the high-intensity absorption band of the solvent. Consequently, this region of the experimental spectrum cannot be compared to the predicted spectrum. The absorption bands in the predicted spectrum show one-to-one correspondence with the absorption bands in the experimental spectrum of **3**. For example, the high-intensity experimental bands at 953 and 1155 cm^{-1} correspond to the analogous high-intensity bands in the predicted spectrum at 946 and 1151 cm^{-1}, respectively.

The significant VCD bands (Figure 4) in the observed VCD spectrum of $(+)_{589}$-**3** at a concentration of 0.086 M can be seen as three bisignate couplets: a couplet with a positive band at 953 cm^{-1} (+) and a negative band at 966 cm^{-1} (−); a second couplet with a negative band at 1115 cm^{-1} and a positive band at 1119 cm^{-1}; a third couplet with a positive band at 1155 cm^{-1} (+) and negative band at 1173 cm^{-1}. The corresponding couplets in the predicted spectrum can be

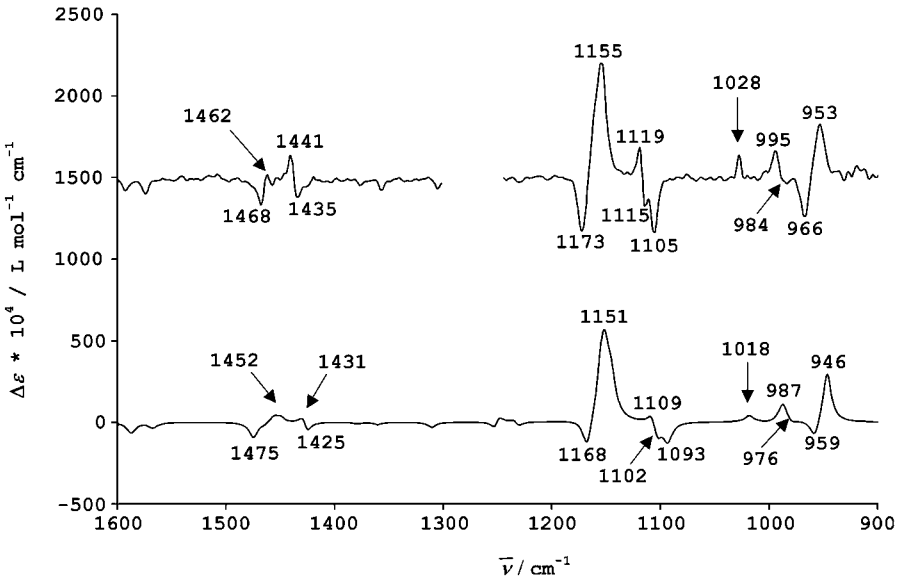

Figure 4. Comparison of the experimental VCD spectrum of (+)-**3** (0.086 M in CH_2Cl_2; path length = 110 μm; obtained as one half of the difference between VCD of (+)- and (−)-enantiomers) with the predicted VCD spectrum (B3LYP/6–31G*) of (*R*)-**3** (top and bottom plots, respectively). Lorentzian band shapes with a half-width at one-half of the peak height of 5 cm^{-1} were used in the spectral simulation; 6–31G* frequencies were scaled by 0.9613.

seen at 946–959 cm^{-1}, 1102–1109 cm^{-1}, and 1151–1168 cm^{-1}, respectively. The vibrational origin of these couplets in the predicted spectrum are as follows: In the first couplet, the positive VCD band at 946 cm^{-1} has contributions from three different vibrations, with the dominant contribution coming from the antisymmetric C–O stretching vibration; the negative band at ~959 cm^{-1} is due to the symmetric C–O stretching vibration. The second couplet originates from phenyl C–H rocking vibrations, with the negative VCD at 1102 cm^{-1} and positive VCD at 1109 cm^{-1} coming, respectively, from symmetric and antisymmetric modes. In the third couplet, the positive VCD band at 1151 cm^{-1} has contributions from five different vibrations, with C–CH_3 stretching and phenyl C–H bending vibrations making major contributions; the negative VCD band at 1168 cm^{-1} originates from C–CH_3 stretching coupled with C–O stretching.

The abovementioned three bisignate VCD features observed for $(+)_{589}$-**3** are reproduced in the predicted VCD spectrum of (*R*)-**3**. The predicted VCD spectrum for (*S*)-**3** would be a mirror image to that of (*R*)-**3** and would not agree with the experimental VCD spectrum for $(+)_{589}$-**3**. The nice agreement seen between the VCD spectra of (*R*)-**3** (predicted) and $(+)_{589}$-**3** (experimental) indicates that the absolute configuration is $(+)_{589}$-(*R*) or, equivalently, $(-)_{589}$-(*S*).

The experimental ECD spectrum obtained for $(-)_{589}$-**3** in CH_2Cl_2 (Figure 5) is similar to that measured by Drabowicz and co-workers[6b] in hexane. The predicted ECD spectrum for (*S*)-**3**, obtained by multiplying the (*R*)-**3** spectrum by −1, is compared to the experimental ECD spectrum of $(-)_{589}$-**3** in Figure 5. Both spectra display an overall positive ECD in the ~210 to 300 nm region, suggesting that the absolute configuration is $(-)_{589}$-(*S*) or, equivalently, $(+)_{589}$-(*R*). The origin of ECD features in spiroselenuranes has not been identified before in the literature. We have analyzed the molecular orbital coefficients obtained in the ECD calculation at B3LYP/6–31G* level and found that all of the first 12 electronic transitions calculated are associated with lone pairs of electrons on either Se or O atoms. The lowest energy electronic transition is associated with lone-pair electrons on selenium atoms.

The predicted ORD for (*S*)-**3**, obtained by multiplying that of (*R*)-**3** by −1, is compared to the corresponding experimental ORD measured in CH_2Cl_2 for $(-)_{589}$-**3** (Figure 6). The experimental specific rotations for $(-)_{589}$-**3** at longer wavelengths are negative, but change sign at ~475 nm and increase in magnitude at shorter wavelengths. The same trend is seen in the predicted values for (*S*)-**3**, although the crossover point in the predicted ORD is different from that in the experimental data because of the inaccuracies in electronic transition wavelengths predicted

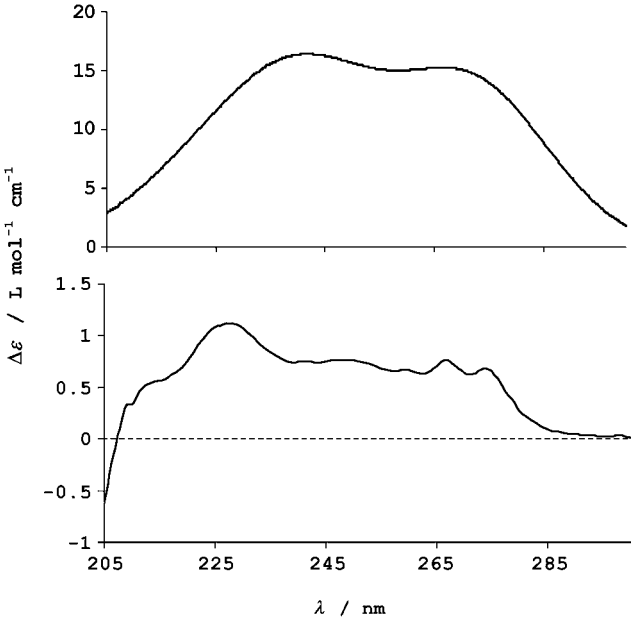

Figure 5. B3LYP/6–31G* predicted ECD spectrum for (*S*)-**3** (top) and experimental ECD spectrum of (−)-**3** (bottom). The theoretical ECD spectrum was simulated using gaussian band shapes with a half-width at 1/e of peak height of 20 nm.

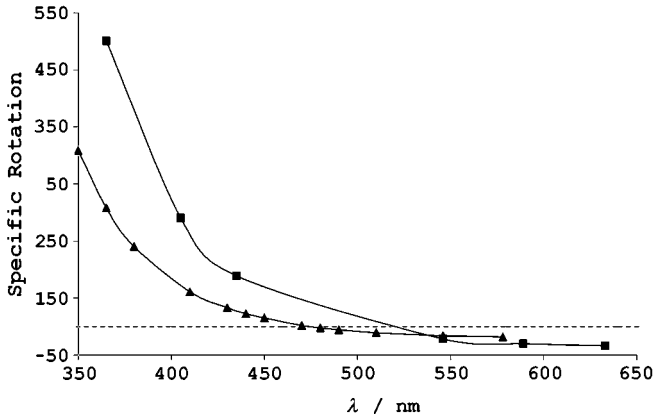

Figure 6. Comparison of ORD predicted data for (*S*)-**3** using B3LYP/6–31G* (■) with experimental data for (−)-**3** (▲).

at B3LYP/6–31G* level. Nevertheless, a nice correlation seen in the trends of predicted and experimental ORD data provides another verification that the absolute configuration of **3** is $(+)_{589}$-(*R*) or $(-)_{589}$-(*S*).

Given that the first eluted enantiomer on a Chiralpack AS analytical column, with 10% IPA and 90% hexane as the mobile phase at room temperature, has negative optical rotation at 589 nm in CH_2Cl_2, it is concluded that the *S* enantiomer of **3** elutes first on this column.

We have also undertaken calculations of VCD, ECD, and ORD with the 6–31+G basis set (and B3LYP functional) and obtained results similar to those in the aforementioned B3LYP/6–31G* calculations, except that the B3LYP/6–31+G calculations did not predict negative optical rotation at longer wavelengths. Given that there is no electronic transition for **3** at 475 nm, the change in sign of rotation at 475 nm can be attributed to the cancellation of opposing ORD contributions from different, shorter-wavelength ECD bands. Such cancellation does not occur quantitatively, unless the ECD intensities at shorter wavelengths are predicted accurately. As one cannot hope to obtain quantitatively accurate ECD intensities at either B3LYP/6–31G* or B3LYP/6–31+G level, it is only necessary to reproduce the overall ORD pattern, rather than the sign of rotation at one particular wavelength. In this regard, the predicted ORD pattern, at both B3LYP/6–31G* and B3LYP/6–31+G levels, is in agreement with the experimentally observed ORD pattern. We have also attempted the VCD, ECD, and ORD calculations using a much larger aug-cc-pVDZ basis set and B3LYP functional. However, the SCF convergence problems, even after using various different options, prevented the completion of these calculations.

It is interesting to note that the absolute configuration for **3**, $(+)_{589}$-(*R*), determined here, is opposite to that determined[6a] for **2**, $(-)_{589}$-(*R*), by using X-ray crystallography, but is the same as that determined[1] for **1**, $(-)_{589}$-(*S*). The ECD spectra of $(-)_{589}$-**3** and $(-)_{589}$-**2** are also significantly different. The chemical constitutional difference between spiroselenuranes **3** and **2**, namely, a lone pair (in **3**) versus an oxygen atom (in **2**) attached to the selenium atom, must be the source for change in the sign of rotation for a given configuration.

Very recently, the absolute configurations of spirosulfurane and spirotellurane with structures analogous to **3** were deduced to be the same as that of **3** [$(+)_{589}$-(*R*) or $(-)_{589}$-(*S*)] on the basis of the dirhodium-NMR method.[19]

Conclusion

Due to its rigid structure, spiroselenurane is stable as a *trans* isomer. The agreement between the theoretical and experimental chiroptical parameters, namely, VCD, ECD, and ORD, leads to the conclusion that the absolute configuration of 3,3,3′,3′-tetramethyl-1,1′-spirobi[3*H*,2,1]benzoxaselenole is $(+)_{589}$-(*R*) and $(-)_{589}$-(*S*), where $(+)_{589}$ and $(-)_{589}$ are the signs of observed rotations at 589 nm in CH_2Cl_2. Given that the first eluted enantiomer on a Chiralpack AS analytical column, with 10% IPA and 90% hexane as the mobile phase at room temperature, has negative optical rotation at 589 nm in CH_2Cl_2, it is concluded that the *S* enantiomer of **3** elutes first on this column. Furthermore, this work demonstrates the first combined use of VCD, ECD, and ORD techniques complementing each other to assign the absolute configurations with increased confidence.

Experimental and Theoretical Methods

Synthesis and resolution: Compound **3** in racemic form has been synthesized at Lodz by means of a one-step reaction[6b] of diethyl selenite and the Grignard reagent derived from orthobromcumyl alcohol. Drabowicz and co-workers[6b] have demonstrated resolution of enantiomers of **3** on a Chiralpack AS column with the first and second eluted enantiomers exhibiting negative {$[\alpha]_D = -20$ ($c = 0.36$, CH_2Cl_2)} and positive {$[\alpha]_D = +21$ ($c = 0.35$, CH_2Cl_2)} rotations, respectively. Following this approach, the enantiomeric separation was carried out at Wyeth laboratories on a Chiralpack AS analytical column (20x250 mm), with 10% IPA and 90% hexane as the mobile phase at room temperature. The separation factor, α, was 1.9, and the resolution factor, R_s, was 2.7. Note that the sign of optical rotation changes at shorter wavelengths and the $(+)_{589}$- and $(-)_{589}$-enantiomers of **3** are identified in this manuscript by their rotation at 589 nm in CH_2Cl_2.

Absorbance and VCD Spectra: The absorption and VCD spectra were recorded at Vanderbilt on a commercial Fourier Transform VCD spectrometer, Chiralir, in the 2000–900 cm^{-1} region. The VCD spectra were recorded with a three-hour data collection time at 4 cm^{-1} resolution. Spectra were measured in CH_2Cl_2 at concentrations of 0.075 M and 0.086 M for $(-)_{589}$- and $(+)_{589}$-enantiomers, respectively. The sample was held in a variable path length cell with BaF_2 windows and a path length of 110 μm. In the absorption spectrum presented, the raw solvent absorption was subtracted out. In the VCD spectrum presented, the VCD spectrum of the solvent was eliminated indirectly by subtracting the VCD spectra of two enantiomers and then scaling the intensities by $^1/_2$.

ECD spectra and ORD: The ECD spectra were recorded on a Jasco J720 spectropolarimeter at Vanderbilt, by using a 0.01-cm path length and CH_2Cl_2, and on a CD6 dichrograph at Lodz, by using a 0.05-mm path length and hexane. The optical rotations at discrete wavelengths were measured in CH_2Cl_2 using an Autopol IV polarimeter at Vanderbilt and with a Perkin–Elmer 241 polarimeter at Lodz.

Calculations: All calculations were done at Vanderbilt. The geometry optimizations, vibrational frequencies, absorption and VCD intensities for spiroselenurane were calculated using the Gaussian 98 program. The calculations were based on the DFT method with B3LYP functional, by using 6–31G* and 6–31+G basis sets. The theoretical absorption and VCD spectra of (*R*)-**3** were simulated with Lorentzian band shapes and a half-width at one-half of the peak height of 5 cm^{-1}. Since the DFT-predicted band positions are higher than the experimental values, the DFT vibrational frequencies were scaled by 0.9613 in the 6–31G* calculation and by 0.9899 in the 6–31+G calculation. The ORD and ECD calculations were undertaken using the same levels of theory as for VCD, by using the Gaussian 03 program. The theoretical ECD intensities, of the first 12 electronic transitions in the 6–31G* calculation and 16 electronic transitions in the 6–31+G calculation, were used to simulate the ECD spectra for (*S*)-**3** using gaussian band shapes and a half-width at 1/e of peak height of 20 nm.

Acknowledgements

This work was supported by a grant (to P.L.P.) from the National Science Foundation (CHE0092922). J.D. thanks JSPS and PAS (for support of the bilateral project "Optically Active Heteroatom Derivatives with Asymmetric Center only at High Coordinated Heteroatoms: New Synthetic Approaches and Comparative Studies on their Racemization"), Dr T. Girek for help in the preparation of the racemic selenurane, and Professors M. Mikolajczyk, Y. Yamamoto, and K-ya. Akiba for helpful discussions.

[1] S. Claeson, V. Langer, S. Allenmark, *Chirality* **2000**, *12*, 71–75.
[2] R. Lesser, R. Weiss, *Ber. Dtsch. Chem. Ges.* **1914**, *47*, 2510–2525.
[3] B. Dahlen, B. Lindgren, *Acta Chem. Scand.* **1973**, *27*, 2218–2220.
[4] F. Ohno, T. Kawashima, R. Okazaki, *Chem. Commun.* **2001**, 463–464.
[5] J. Zhang, S. Takahashi, N. Sato, T. Koizumi, *Tetrahedron: Asymmetry* **1998**, *9*, 3303–3317.
[6] a) J. Drabowicz, J. Luczak, M. Mikolajczyk, Y. Yamamato, S. Matsukawa, K. Akiba, *Chirality* **2004**, *16*, 598–601; b) J. Drabowicz, J. Luczak, M. Mikolajczyk, Y. Yamamato, S. Matsukawa, K. Akiba, *Tetrahedron: Asymmetry* **2002**, *13*, 2079–2082.
[7] a) L. D. Barron, *Molecular Light Scattering and Optical Activity*, 2nd ed., Cambridge University Press, Cambridge, **2004**; b) P. L. Polavarapu, *Vibrational Spectra: Principles and Applications with Emphasis on Optical Activity*, Elsevier, New York, **1998**; c) T. B. Freedman, X. Cao, R. K. Dukor, L. A. Nafie, *Chirality* **2003**, *15*, 743–758.
[8] J. R. Cheeseman, M. J. Frisch, F. J. Devlin, P. J. Stephens, *Chem. Phys. Lett.* **1996**, *252*, 211.
[9] Gaussian 98, M. J. Frisch, G. W. Trucks, H. B. Schlegel, G. E. Scuseria, M. A. Robb, J. R. Cheeseman, V. G. Zakrzewski, J. A. Montgomery, R. E. Stratmann, J. C. Burant, S. Dapprich, J. M. Millam, A. D. Daniels, K. N. Kudin, M. C. Strain, O. Farkas, J. Tomasi, V. Barone, M. Cossi, R. Cammi, B. Mennucci, C. Pomelli, C. Adamo, S. Clifford, J. Ochterski, G. A. Petersson, P. Y. Ayala, Q. Cui, K. Morokuma, D. K. Malick, A. D. Rabuck, K. Raghavachari, J. B. Foresman, J. Cioslowski, J. V. Ortiz, B. B. Stefanov, G. Liu, A. Liashenko, P. Piskorz, I. Komaromi, R. Gomperts, R. L. Martin, D. J. Fox, T. Keith, M. A. Al-Laham, C. Y. Peng, A. Nanayakkara, C. Gonzalez, M. Challacombe, P. M. W. Gill, B. G. Johnson, W. Chen, M. W. Wong, J. L. Andres, M. Head-Gordon, E. S. Replogle, J. A. Pople, Gaussian, Inc., Pittsburgh, PA, **1998**; Gaussian 03, M. J. Frisch, G. W. Trucks, H. B. Schlegel, G. E. Scuseria, M. A. Robb, J. R. Cheeseman, J. A. Montgomery, Jr., T. Vreven, K. N. Kudin, J. C. Burant, J. M. Millam, S. S. Iyengar, J. Tomasi, V. Barone, B. Mennucci, M. Cossi, G. Scalmani, N. Rega, G. A. Petersson, H. Nakatsuji, M. Hada, M. Ehara, K. Toyota, R. Fukuda, J. Hasegawa, M. Ishida, T. Nakajima, Y. Honda, O. Kitao, H. Nakai, M. Klene, X. Li, J. E. Knox, H. P. Hratchian, J. B. Cross, V. Bakken, C. Adamo, J. Jaramillo, R. Gomperts, R. E. Stratmann, O. Yazyev, A. J. Austin, R. Cammi, C. Pomelli, J. W. Ochterski, P. Y. Ayala, K. Morokuma, G. A. Voth, P. Salvador, J. J. Dannenberg, V. G. Zakrzewski, S. Dapprich, A. D. Daniels, M. C. Strain, O. Farkas, D. K. Malick, A. D. Rabuck, K. Raghavachari, J. B. Foresman, J. V. Ortiz, Q. Cui, A. G. Baboul, S. Clifford, J. Cioslowski, B. B. Stefanov, G. Liu, A. Liashenko, P. Piskorz, I. Komaromi, R. L. Martin, D. J. Fox, T. Keith, M. A. Al-Laham, C. Y. Peng, A. Nanayakkara, M. Challacombe, P. M. W. Gill, B. Johnson, W. Chen, M. W. Wong, C. Gonzalez, J. A. Pople, Gaussian, Inc., Wallingford CT, **2004**; Dalton, A Molecular Electronic Structure Program, University of Oslo, Norway, **2001**.
[10] a) P. L. Polavarapu, *Mol. Phys.* **1997**, *91*, 551–554; b) P. L. Polavarapu, *Chirality* **2002**, *14*, 768–781; P. L. Polavarapu, *Chirality* **2003**, *15*, 284–285.
[11] a) M. Pecul, K. Ruud, A. Rizzo, T. Helgaker, *J. Phys. Chem. A* **2004**, *108*, 4269–4276; b) M. C. Tam, N. J. Russ, T. D. Crawford, *J. Chem. Phys.* **2004**, *121*, 3550–3557; c) T. B. Pedersen, H. Koch, L. Boman, A. M. J. Sanchez de Meras, *Chem. Phys. Lett.* **2004**, *393*, 319–326; d) E. Giorgio, C. Minichino, R. G. Viglione, R. Zanasi, C. Rosini, *J. Org. Chem.* **2003**, *68*, 5186–5192; e) S. Grimme, A. Bahlmann, G. Haufe, *Chirality* **2002**, *14*, 793–797; f) M. Goldsmith, N. Jayasuri, D. N. Beratan, P. Wipf, *J. Am. Chem. Soc.* **2003**, *125*, 15696–15697; g) K. B. Wiberg, Y. Wang, P. H. Vaccaro, J. R. Cheeseman, G. Trucks, M. J. Frisch, *J. Phys. Chem. A* **2004**, *108*, 32–38; h) B. Mennucci, J. Tomasi, R. Cammi, J. R. Cheeseman, M. J. Frisch, F. J. Devlin, S. Gabriel, P. J. Stephens, *J. Phys. Chem. A* **2002**, *106*, 6102–6113.
[12] a) P. L. Polavarapu, C. Zhao, *J. Am. Chem. Soc.* **1999**, *121*, 246–247; b) K. M. Specht, J. Nam, D. M. Ho, N. Berova, R. K. Kondru, D. N. Beratan, P. Wipf, R. A. Pascal, Jr., D. Kahne, *J. Am. Chem. Soc.* **2001**, *123*, 8961–8966; c) P. L. Polavarapu, *Angew. Chem.* **2002**, *114*, 4726–4728; *Angew. Chem. Int. Ed.* **2002**, *41*, 4544–4546; d) P. Norman, K. Ruud, T. Helgaker, *J. Chem. Phys.* **2004**, *120*, 5027–5035; e) J. Crassous, Z. Jiang, V. Schurig, P. L. Polavarapu, *Tetrahedron: Asymmetry* **2004**, *15*, 1995–2001; f) E. Giorgio, R. G. Viglione, R. Zanasi, C. Rosini, *J. Am. Chem. Soc.* **2004**, *126*, 12968–12976; g) T. D. Crawford, L. S. Owens, M. C. Tam, P. R. Schreiner, H. Koch, *J. Am. Chem. Soc.* **2005**, *127*, 1368–1369.
[13] a) C. Diedrich, S. Grimme, J. *Phys. Chem. A* **2003**, *107*, 2524–2539; b) M. Pecul, K. Ruud, T. Helgaker, *Chem. Phys. Lett.* **2004**, *388*, 110–119; c) T. B. Pedersen, H. Koch, K. Ruud, *J. Chem. Phys.* **1999**, *110*, 2883–2892; d) F. Furche, R. Ahlrichs, C. Wachsmann, E. Weber, A. Sobanski, F. Vogtle, S. Grimme, *J. Am. Chem. Soc.* **2000**, *122*, 1717–1724; e) P. J. Stephens, D. M. McCann, E. Buktus, S. Stoncius, J. R. Cheeseman, M. J. Frisch, *J. Org. Chem.* **2004**, *69*, 1948–1958.
[14] B. Testa, *Principles of Organic Stereochemistry*, Marcel Dekker, New York, **1979**.
[15] D. Nasipuri, *Stereochemistry of Organic Compounds*, Wiley Eastern Limited, New Delhi, **1991**.
[16] N. Harada, K. Nakanishi, *Circular Dichroic Spectroscopy: Excition Coupling in Organic Stereochemistry*, University Science Books, Mill Valley, **1983**.
[17] R. S. Cahn, C. K. Ingold, V. Prelog, *Angew. Chem.* **1966**, *78*, 413–447; *Angew. Chem. Int. Ed. Engl.* **1966**, *5*, 385–419.
[18] J. C. Martin, T. M. Balthazor, *J. Am. Chem. Soc.* **1977**, *99*,152–162.
[19] T. Gáti, G. Tóth, J. Drabowicz, S. Moeller, E. Hofer, H. Duddeck, *Chirality* **2005**, *17*, S40-S47.

Received: December 23, 2004
Published online: May 2, 2005